

Regular Article

Survival Motor Neuron Protein Modulates Lysosomal Function Through the Expression of Transcription Factor EB in Motoneurons

Shiori Ando,^a Wataru Otsu,^{*b} Daiki Osanai,^a Satoshi Kamiya,^a Kodai Ishida,^b Shinsuke Nakamura,^a Masamitsu Shimazawa,^{a,b} and Hideaki Hara^{a,b}

^aMolecular Pharmacology, Department of Biofunctional Evaluation; ^bDepartment of Biomedical Research Laboratory, Gifu Pharmaceutical University, 1-25-4 Daigaku-nishi, Gifu, 501-1196, Japan

Received July 3, 2020; Accepted July 30, 2020

Spinal muscular atrophy (SMA) is a progressive neuromuscular disease, associated with motoneuron loss and muscle wasting. Numerous SMA-causative mutations have been reported in survival motor neuron (SMN) gene(s); however, the pathogenic mechanism underlying SMA remains unclear. In the present study, we showed that SMN modulates the expression of transcription factor EB (TFEB), a master regulator of lysosomal genes that plays a key role in lysosome function, autophagy, and the mammalian target of rapamycin (mTOR) signaling pathway. The transfection of small interfering RNA (siRNA) targeting SMN caused a reduction in TFEB expression in the motoneuron-like NSC-34 cell line. In differentiated NSC-34 cells, either SMN or TFEB knockdown resulted in reduced lysosomes at neurites and the atypical accumulation of swollen and enlarged lysosomes in cell bodies. SMN knockdown caused the reduced expression of lysosome-related genes, resulting in the decline of lysosomal degradation and increased autophagic flux. These SMN-depletion-induced aberrations in lysosomes and autophagy could be rescued by the exogenous expression of TFEB. Furthermore, SMN depletion in NSC-34 cells resulted in the decreased phosphorylation of mTOR and its downstream signals. Finally, SMA transgenic mice exhibited reduced TFEB and lysosomal protein expression and the inactivation of mTOR signaling in the lumbar spinal cord at postnatal day 11, compared with their counterparts. These findings indicated that SMN regulates lysosomal gene expression and functions by altering TFEB expression in motoneurons. The targeting of lysosomes might represent a new strategy for the treatment of SMA.

Key words spinal muscular atrophy, survival motor neuron, transcription factor EB, lysosome, NSC-34 cells

INTRODUCTION

Spinal muscular atrophy (SMA) is an autosomal recessive, neurodegenerative disorder, characterized by the selective loss of motoneurons in the spinal cord.¹⁾ Numerous deletion and point mutations in *survival motor neuron gene-1 (SMN1)* have been reported, after it was identified as a causative gene for SMA.²⁾ Human genomes contain a copy gene, *SMN2* (over 99% identical to *SMN1*), which produces less than 10% functional, full-length SMN protein, due to a point mutation in exon 7.^{3,4)} The copy number of *SMN2* has been inversely correlated with the severity of pathological symptoms and defects in neuromuscular junctions (NMJs).²⁾ The well-described functions of SMN include the biogenesis of spliceosomal small nuclear ribonucleoprotein particles (snRNPs) and the axonal delivery of RNA.^{5,6)} SMN protein is degraded by the ubiquitin-proteasome system and autophagy.^{7,8)} However, the role played by SMN in lysosomes has been less well-investigated.

Lysosomes are intracellular, acidic organelles that play a central role in the degradation of endocytosed extracellular materials and cell surface receptors and nutrient metabolism.^{9,10)} Transcription factor EB (TFEB) is a master regulator of the coordinated lysosomal expression and regulation (CLEAR) network, which regulates the transcription of genes

associated with lysosomes and autophagy.¹¹⁾ The interaction between TFEB and mammalian target of rapamycin (mTOR) plays an essential role in the regulation of catabolic processes and autophagy under starvation conditions.^{12,13)} Amino acid signaling promotes the recruitment of mTOR complex 1 to the lysosomal surface, resulting in the activation of the mTOR downstream pathway, such as ribosomal protein S6 kinase beta-1 (also known as p70S6 kinase, p70S6K) and S6 ribosomal protein (S6RP), which are involved in protein synthesis.¹⁴⁾ The dysregulation of mTOR has been shown to be involved in SMA pathophysiology.¹⁵⁾ In addition, TFEB has been shown to be selectively reduced in the brains of amyotrophic lateral sclerosis (ALS) and Alzheimer's disease patients.¹⁶⁾ Moreover, TFEB function has been reported to be disrupted by the polyglutamine-expanded androgen receptor, which causes spinal and bulbar muscular atrophy (SBMA).¹⁷⁾ These findings indicate the important role played by TFEB in motoneurons and suggest a possible link between TFEB dysfunction and neurodegenerative diseases, including SMA.

Here, we investigated the link between TFEB and SMN, using *in vitro* NSC-34 cell cultures and an *in vivo* SMA model animal. SMN knockdown (KD) reduced TFEB expression, at both the mRNA and protein levels. Concomitantly, SMN-depleted cells displayed reduced lysosome-related gene expression, lysosome dysfunction, and increased autophagy

*To whom correspondence should be addressed. e-mail: otsu-wa@gifu-pu.ac.jp

influx. Furthermore, SMN depletion resulted in the decreased phosphorylation of mTOR and its downstream effectors, p70S6K and S6RP. Finally, reduced TFEB and lysosomal protein expression and the inactivation of mTOR signaling were identified in the spinal tissue of SMA transgenic mice. These findings provided new insights into the roles played by TFEB and lysosomes in SMA etiology.

MATERIALS AND METHODS

Reagents The primary antibodies used were as follows; SMN [mouse, BD Biosciences, Franklin Lakes, NJ, USA, Cat# 610647, 1:10,000 for immunoblotting (IB)], TFEB [rabbit, Proteintech, Rosemont, IL, USA, Cat# 13372-1-AP, 1:5,000 for IB, 1:200 for immunofluorescence (IF)], β -actin (mouse, Sigma-Aldrich, St. Louis, MO, USA, Cat# A2228, 1:100,000 for IB), Lamp1 (rat, Abcam, Cambridge, UK, Cat# 1b25245, 1:10,000 for IB, 1:400 for IF), β -Tubulin III (rabbit, Gene-Tex Inc., Irvine, CA, USA, Cat# GTX130245, 1:2,000 for IF), cathepsin D (goat, R&D Systems, Minneapolis, MN, USA, Cat# AF1029-SP, 1:5,000 for IB), microtubule-associated protein light chain 3 (LC3B, rabbit, GeneTex, Cat# GTX127375, 1:10,000 for IB), p-mTOR (Ser 2448, rabbit, Cell Signaling Technology, Danvers, MA, USA, Cat# 2971S, 1:10,000 for IB), mTOR (rabbit, Cell Signaling Technology, Cat# 2972S, 1:10,000 for IB), p-p70S6K (rabbit, Cell Signaling Technology, Cat# 9234S, 1:500 for IB), p70S6K (rabbit, Cell Signaling Technology, Cat# 9202S, 1:1,000 for IB), p-S6RP (rabbit, Cell Signaling Technology, Cat# 4856S, 1:1,000 for IB), S6RP (rabbit, Cell Signaling Technology, Cat# 2317S, 1:2,000 for IB), green fluorescent protein (GFP, rabbit, MBL Life Science, Aichi, Japan, 1:50,000 for IB).

Alexa-dye conjugated secondary antibodies were purchased from Thermo Fisher Scientific (Waltham, MA, USA, 1:400 for IF). Horseradish peroxidase (HRP)-conjugated secondary antibodies were purchased from Thermo Fisher Scientific (1:10,000 for IB). Small interfering RNAs (siRNAs) targeting *Smn* (siSMN#1, Cat# Smn1MSS209213; siSMN#2, Cat# Smn1MSS209214), *Tfeb* (siTFEB#1, Cat# TfebMSS238271; siTFEB#2, Cat# TfebMSS238272), and a negative control (Cat# 12935300), were purchased from Thermo Fisher Scientific. pEGFP-N1-TFEB was purchased from Addgene [Watertown, MA, USA, Addgene plasmid# 38119, gifted by Shawn Ferguson¹²]. pAcGFP-C1 vector was purchased from Takara Bio (Shiga, Japan, Cat# CLN632470).

Cell Culture and Transfection Murine motoneuron-like cells (NSC-34) were purchased from Cosmo Bio Co., Ltd. (Tokyo, Japan) and maintained in Dulbecco's modified Eagle's medium (DMEM, Nacalai Tesque, Kyoto, Japan), containing 10% fetal bovine serum (FBS, Valeant, Costa Mesa, CA), as described previously.¹⁸ Lipofectamine RNAiMAX and Lipofectamine 2000 were used as transfection reagents, according to the manufacturer's instructions (Thermo Fisher Scientific). To induce differentiation, one day after seeding into 6-well plates, at 20,000 cells per wells, NSC-34 cells were incubated with DMEM, containing 50 μ M *all-trans* retinoic acid (Sigma-Aldrich, Cat# R2625) and 2% horse serum (Sigma-Aldrich, Cat# H1138), for 3 days, in a humidified atmosphere of 95% air and 5% CO₂ at 37°C. The percentage of neurite-bearing cells reached to 57.7 \pm 9.3% on the day 3.

Cell Lysis and Immunoblotting Cell lysis and immunoblotting were performed, as previously described.¹⁹ Brief-

ly, cells cultured in a 12-well plate were rinsed with ice-cold PBS and lysed in radioimmunoprecipitation assay (RIPA) buffer (Sigma-Aldrich, R0278), containing protease inhibitor cocktail, and phosphatase inhibitor cocktail 2 and 3 (Sigma-Aldrich), and then centrifuged at 12,000 \times g, for 20 min at 4°C. The supernatants were collected as cell lysates and boiled with sample buffer solution (FUJIFILM-Wako, Osaka, Japan), for 5 min. Protein extracts were separated by sodium dodecyl sulfate-polyacrylamide gel electrophoresis (SDS-PAGE), in a 5%–20% gradient gel (SuperSep Ace, FUJIFILM-Wako), and transferred to a polyvinylidene difluoride membrane (Immobilon-P, Millipore, Bedford, MA, USA). After blocking with Blocking One-P (Nacalai Tesque), the membranes were incubated with primary antibody, in Can Get Signal Solution-1 (Toyobo, Shiga, Japan), overnight at 4°C, with gentle agitation. After three washes with Tris-buffered saline (TBS), containing 0.05% Tween 20, the membranes were incubated with an HRP-conjugated secondary antibody, in Can Get Signal Solution-2 (Toyobo), for 1 h at room temperature. After three washes with TBS, containing 0.05% Tween 20, the chemiluminescent signal was visualized with ImmunoStar LD (Fujifilm-Wako) and then detected using an Amersham Imager 680 (GE Lifescience, Chicago, IL, USA). The band intensity was analyzed by Amersham Imager 680 Analysis Software (GE Lifescience).

Quantitative RT-PCR Quantitative reverse transcriptase-polymerase chain reaction (RT-PCR) was performed, as described previously.²⁰ In brief, total RNA was purified from NSC-34 cells, grown in a 12-well plate (Corning), using NucleoSpin RNA (Takara Bio), and subjected to reverse transcription to generate a cDNA library, using Prime-Script RT reagent Kit (Takara Bio). Quantitative RT-PCR was performed on a Thermal Cycler Dice Real-Time System III (Takara Bio), using TB Green Premix Ex Taq II (Takara Bio). The primer pairs used in this study were as follows; Gapdh-F, 5'-AACTTTGGCATTGTGGAA-GG-3'; Gapdh-R 5'-ACACATTGGGGGTAGGAACA-3'; Tfeb-F, 5'-TCAGAAGCGAGAGCTAACAGAT-3'; Tfeb-R 5'-TGTGATTGTCTTTCTTCTGCCG-3'; Lamp1-F, 5'-CAGCACTCTTTGAGGTGAAAAAC-3'; Lamp1-R 5'-ACGATCTGAGAACCATTTCGCA-3'; Ctsd-F, 5'-GCTTC-CGGTCTTTGACAACCT-3'; and Ctsd-R, 5'-CACCAA-GCATTAGTTCTCCTCC-3'. C_T values measured Thermal Cycler Dice Real-Time System software (Takara Bio) by were normalized against Gapdh and expressed as the fold-change in gene expression.

Immunostaining Immunostaining was performed as previously described, with minor modifications.²¹ Briefly, cells were grown on 12-mm glass coverslips (No. 1-S, Matsunami Glass Industry, Osaka, Japan), coated with 0.2% gelatin, from porcine skin (Sigma Aldrich, G2500), and fixed with 4% paraformaldehyde (Electron Microscopy Sciences, Fort Washington, PA) in PBS-C/M [phosphate-buffered saline (PBS), containing 0.2 mM CaCl₂, 2 mM MgCl₂], for 10 min at room temperature, quenched with 50 mM NH₄Cl, for 10 min, followed by 30 min in blocking buffer [PBS-C/M containing 0.5% bovine serum albumin (BSA), 0.5% saponin, 0.2 mg/ml sodium azide]. The samples were incubated with primary antibodies in PBS-C/M, for 1 h. After three washes with PBS-C/M, cells were stained with secondary antibodies in PBS-C/M, containing 8.1 μ M Hoechst 33342 (Thermo Fisher

Scientific), for 30 min. For F-actin staining, the samples were stained with Phalloidin-iFluor 594 (Cayman Chemical, Ann Arbor, MI, USA, 1:2,000) together with the secondary antibody. After three washes with PBS-C/M, the coverslips were mounted with ProLong Gold Antifade reagent (Thermo Fisher Scientific). Images were acquired, using either a 40× or 100× objective lens, on a Zeiss LSM700 microscope (Carl Zeiss, Germany). Images were edited using ImageJ (National Institutes of Health) or Adobe Photoshop CC2019 (Adobe), for presentation purposes. To analyze TFEB foci-positive cell ratios, images were analyzed by a third person, in a blinded fashion.

DQ-Red BSA Lysosomal Activity Assay The DQ-Red BSA (Thermo Fisher Scientific) assay was performed, according to the manufacturer's instructions. Briefly, cells were incubated with 10 µg/ml DQ-Red BSA, for 3 h at 37°C. Hoechst 33342 solution was added, 15 min before recording, to a final concentration of 8.1 µM. For live-cell imaging, the medium was changed to Live Cell Imaging Solution (LCIS, Thermo Fisher Scientific), containing 5.5 mM glucose and 1% FBS, and then images were acquired, using a 10× objective lens on a Lionheart FX Automated Microscope (Bio Tek Instruments, Winooski, VT, USA). The obtained images were analyzed by Gen5 software (Bio Tek Instruments).

Animal Experiments SMNΔ7 mice (*mSmn*^{-/-}, *SMN2*^{+/+}, *SMNΔ7*^{+/+}) were purchased from Jackson Laboratory (Bar Harbor, ME, USA, Stock Number 005025) and maintained, as described previously.¹⁹ Lumbar spinal cords, from either SMNΔ7 mice or their wild-type (WT) counterparts (*mSmn*^{+/+}, *SMN2*^{+/+}, *SMNΔ7*^{+/+}), were harvested at postnatal day 11 and homogenized, using Physcotron (Microtec Co., Chiba, Japan) in RIPA buffer, containing protease inhibitor cocktail, and phosphatase inhibitor cocktail 2 and 3 (Sigma-Aldrich), then centrifuged, at 12,000 × g, for 20 min at 4°C. The supernatants were examined by immunoblotting, as tissue lysates. All animal manipulations were performed in accordance with the animal care guidelines issued by the National Institutes of Health. All experiments were approved by the Institutional Animal Care and Use Committee of Gifu Pharmaceutical University (Approval No. 2019-078, 2019-190).

Statistical Analysis All data are presented as the mean ± standard error of the mean (S.E.M.). Statistical analyses were performed by Student's *t*-tests, using SPSS Statistical Software (IBM, Armonk, NY, USA).

RESULTS

NSC-34 cells, a motoneuron-like hybrid cell line, have been used as an *in vitro* model because of their physiological properties.²² To silence SMN expression in NSC-34 cells, two siRNAs, targeting different regions of *Smn*, were validated by immunoblotting (Fig. S1A and B). The expression of SMN was significantly decreased, 24 h after transfection, and reduced expression persisted until 72 h after transfection (Fig. 1A and B). Coincidentally, we found that TFEB expression also decreased 48 h and 72 h after transfection (Fig. 1A and C). The mRNA levels of *Tfeb* also decreased at the 48 h time point (Fig. 1D), suggesting that the transcription of TFEB was suppressed by SMN KD. At steady state, TFEB exists in the cytosol, and activated TFEB is shuttled into the nucleus, to promote lysosomal gene expression.¹¹ In control NSC-34 cells, endogenous TFEB staining appeared as bright cytosol-

ic foci, in addition to signals in the nuclei (Fig. 1E). Consistent with the immunoblotting and quantitative RT-PCR results, TFEB-positive foci disappeared in SMN-depleted cells (Fig. 1E and F). These foci were diminished following the transfection of siRNA targeting TFEB expression (Fig. S2A-C), suggesting that these signals were neither background nor artifacts.

All-trans retinoic acids can induce the differentiation of NSC-34 cells.²³ We performed immunostaining against the lysosomal marker Lamp1, in differentiated NSC-34 motoneurons (Fig. 2A) because TFEB is important for lysosomal biogenesis and distribution. Differentiated NSC-34 cells displayed long processes, which could be labeled by the neuronal marker β-tubulin III (Fig. 2B–D). The membranes of the neurite branches were highlighted by F-actin staining, and the distal regions of the neurites were enriched with Lamp1-positive granular structures (Fig. 2B, asterisks). Interestingly, these structures disappeared in both SMN KD and TFEB KD cells (Fig. 2C and D). Instead, we found that lysosomes became swollen and enlarged, and these irregularly shaped lysosomes accumulated in the cell bodies (soma) of KD cells (Fig. 2C and D). The shapes of lysosomes have been associated with acidity and degradation.²⁴ Therefore, these results indicate that lysosomal function was disrupted by SMN KD.

TFEB regulates lysosome-related gene expression.¹¹ As expected, the mRNA levels of both Lamp1 and cathepsin D (CTSD) were reduced in SMN KD cells (Fig. 3A). Consistently, the protein levels of Lamp1 and CTSD were reduced at the 72 h time point (Fig. 3B–D). Along with lysosomes, TFEB also regulates autophagic gene expression and the induction of autophagy.²⁵ Immunoblotting for LC3 revealed that SMN KD increased autophagic flux (Fig. 3B and E). To investigate the lysosomal activity, we performed the DQ-Red BSA assay. SMN KD cells showed reduced DQ-Red BSA fluorescence intensity compared with that of control cells (Figs. 3F and S3A). Taken together, these results indicated that SMN expression is essential for maintaining lysosome level, its degradation and autophagic activity in motoneurons.

To exclude the possibility that SMN KD directly suppresses the expression of lysosome-related genes, we performed a rescue experiment, in which we transiently expressed exogenous TFEB in SMN-depleted cells (Fig. 4A). Indeed, the exogenous expression of TFEB ameliorated the LC3 ii/i ratio (Fig. 4B and C) and increased the expression of Lamp1 (Fig. 4B and D) but did not affect the expression of SMN, suggesting that TFEB is downstream of SMN. Consequently, the lysosomal and autophagy defects observed in SMN KD cells were likely mediated by decreased TFEB expression.

Lysosomes play a key role in the mTOR signaling pathway.¹⁴ Axonal translation mTOR activity has been reported to be inhibited by miR-183 in SMN KD primary neurons.²⁶ Consistent with previous reports, SMN KD decreased mTOR phosphorylation (Fig. 5A and B). In addition to mTOR, the phosphorylation of both p70S6K and S6RP was also reduced under the same conditions (Fig. 5C and D). Although SMN KD causes apoptosis in NSC-34 cells,²⁷ defects in the mTOR signaling pathway would also contribute to the loss of motoneurons in SMA.

To further investigate motoneurons in the spinal cord, we used SMNΔ7 mice (*mSmn*^{-/-}, *SMN2*^{+/+}, *SMNΔ7*^{+/+}), as an SMA animal model.^{19,28} The lumbar spinal cords were harvested at postnatal day 11. TFEB and Lamp1 levels were significantly

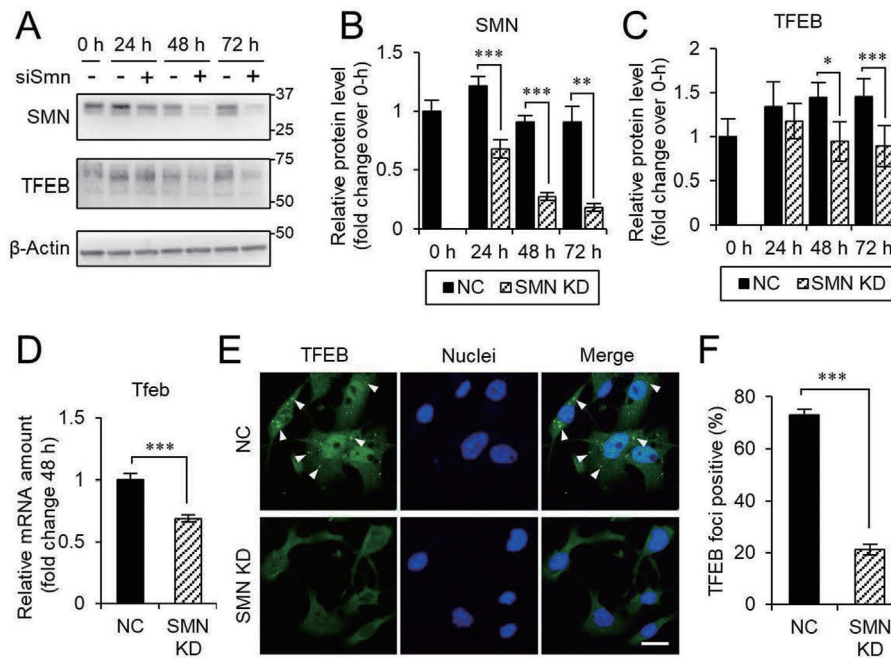


Fig. 1. TFEB Expression Levels Decrease in SMN-Depleted NSC-34 Motoneuron-Like Cells

(A-C) Immunoblotting of cell lysates, obtained from NSC-34 cells, transfected with either negative control RNA (- or NC) or siRNA against SMN (siSmn + or SMN KD), for the indicated times. Representative images of the blots are shown in A. The quantitation of SMN (B) and TFEB (C) signals were normalized against β -actin and are shown the fold-change compared with 0 h. (D) The mRNA level of *Tfeb*, at the 48 h time point, normalized against *Gapdh*. (E) Immunostaining for TFEB (green), in SMN KD cells. Nuclei are stained with Hoechst 33342 (blue). Arrowheads represent TFEB-positive foci. Bar = 20 μ m. (F) The ratio of TFEB foci-positive cells, in either NC or SMN KD. N = 6, mean \pm S.E.M. * P < 0.05, ** P < 0.005, *** P < 0.001 Student's *t*-test vs NC.

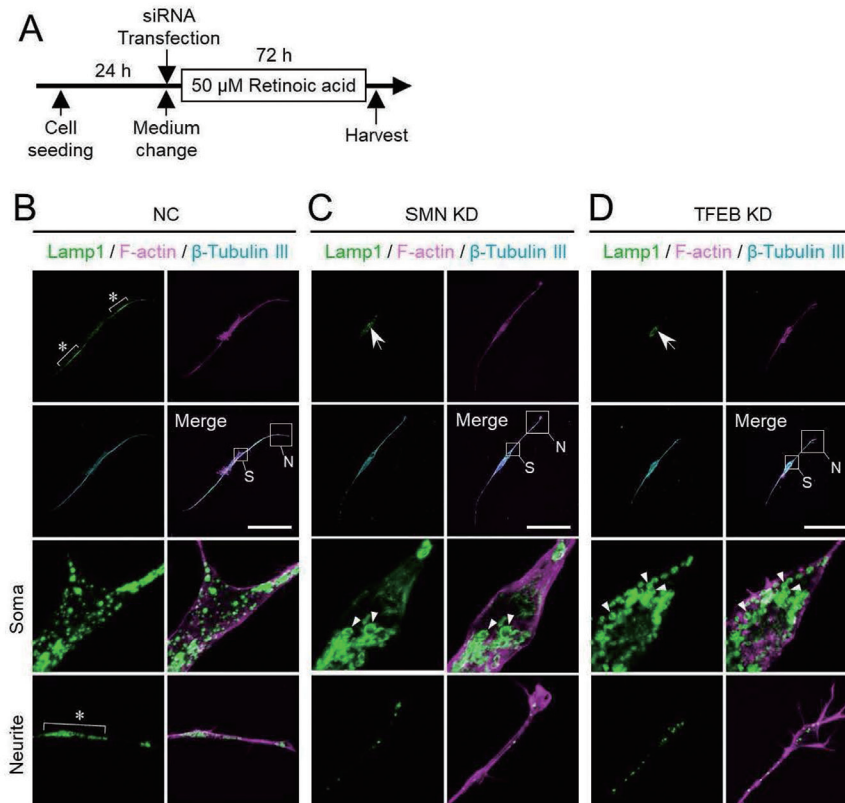


Fig. 2. SMN and TFEB KD Alter the Distribution and Morphology of Lysosomes in Differentiated NSC-34 Cells

(A) A schematic diagram for the timeline of transfection and induction. NSC-34 cells were differentiated by treatment with *all-trans* retinoic acid, after transfection with siRNA against either SMN or TFEB or negative control RNA (NC). (B-C) Representative images of immunostaining against Lamp1 (green, top left), F-actin (magenta, top right), β -Tubulin III (cyan, second lane left), and Hoechst 33342 (blue). The boxed regions at the soma (S) and neurites (N) are enlarged in the third and bottom rows, respectively. Asterisks and arrows represent lysosomes at the neurites and soma, respectively. Arrowheads indicate the abnormal structures of lysosomes. Bars = 100 μ m.

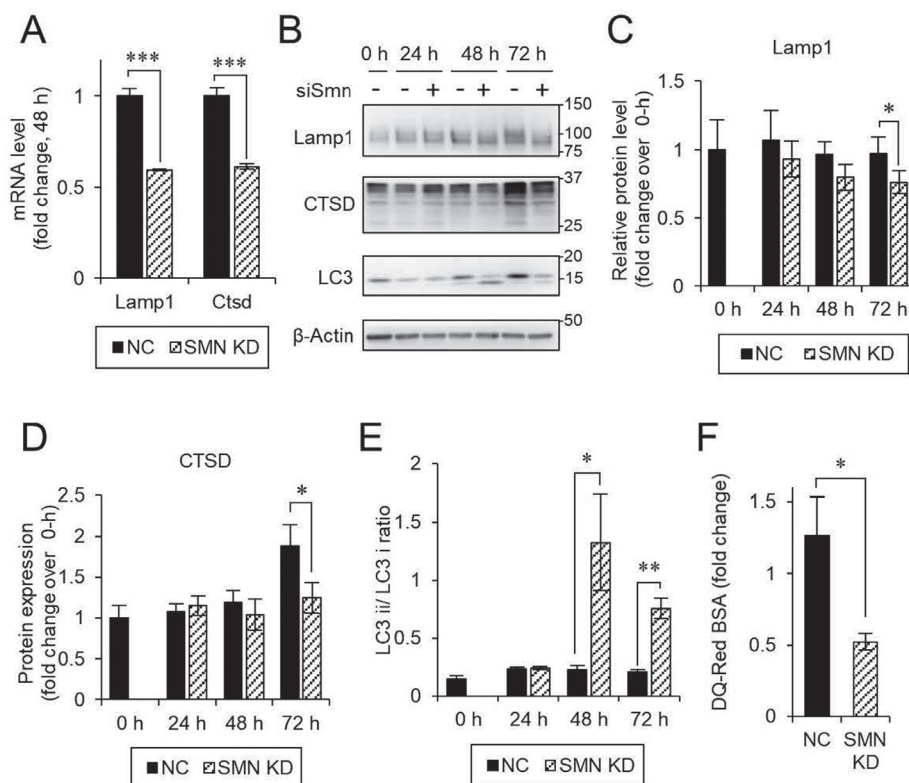


Fig. 3. SMN KD Affects Lysosome-Related Gene Expression, Lysosomal Degradation, and Autophagy Flux

(A) The mRNA levels of *Lamp1* and *Ctsd* at the 48 h time point, normalized against *Gapdh*. (B) Immunoblotting of NSC-34 cell lysates, transfected with either negative RNA (- or NC) or siRNA against SMN (siSmn + or SMN KD), for the indicated time points. (C-E) The quantification of B. The signals for Lamp1 (C) and CTSD (B) were normalized against that for β -actin and are shown as the fold-change relative to the level at 0 h. (E) The ratio of LC3-ii (lower band) vs LC3-i (upper band). (F) The fluorescent intensity of DQ-Red BSA in NSC-34 cells, transfected with negative control or siSmn siRNA, for 72 h, shown as the fold-change vs non-transfected cells. N = 6, mean \pm S.E.M. * P < 0.05, *** P < 0.001 Student's *t*-test vs NC.

decreased in SMN Δ 7 mice (Fig. 6A-C), compared with their counterparts. As well as mTOR, the phosphorylation of S6RP was drastically reduced in SMN Δ 7 mice (Fig. 6D-F). Interestingly, in addition to the reduced phosphorylated form, the total level of S6K was decreased in SMN Δ 7 mice (Fig. 6 D-F). In summary, SMN plays a crucial role in the expression of lysosome-related genes and mTOR signaling pathways in spinal cords, *in vivo*.

DISCUSSION

In the present study, we investigated the functional interaction between SMN and TFEB, in motoneurons. SMN KD reduced TFEB expression, at the transcriptional level (Fig. 1). In addition to a reduction in lysosome-related gene expression, the lysosome dysfunction and increased autophagy influx were observed in SMN-depleted cells (Fig. 3). Consistent with the results obtained from NSC-34 cells, defects in the TFEB and mTOR pathway were detected in the lumbar spinal cords of SMA model mice (Fig. 6). The decline in lysosomes and autophagy was rescued by exogenously expressed TFEB (Fig. 4). Therefore, the reduced intracellular degradation caused by SMN depletion is mediated by the loss of TFEB expression. Previous report showed that caspase-3 activity significantly increased at 72 h after post transfection of *SMN* siRNA in NSC-34 cells²⁷, whereas we found that TFEB level was already declined at an earlier time point 48 h, suggesting that

TFEB down regulation can occur prior to apoptosis. Further study remains necessary to clarify the molecular mechanisms involved in the SMN regulation of TFEB expression and the correlation between TFEB mediated pathway and motoneuron loss.

Intriguingly, we found that the distribution and morphology of lysosomes were altered in SMN-depleted cells (Fig. 2). The endocytic pathway and the degradation of endocytosed components are essential for neurotransmitter secretion and the maintenance of synaptic plasticity.²⁹ Axonal lysosomes and macroautophagy have been reported to play important roles in axonal development.^{30,31} Lysosomal activity is also involved in trans-synaptic communications at the NMJ.³² Motoneurons have long axons; thus, the delivery of lysosomes might be crucial for their survival. TFEB has been associated with the intracellular distribution of lysosomes, by regulating their delivery.³³ Understanding the molecular mechanism associated with the axonal delivery of lysosomes might be a key to understanding the sensitivity of motoneurons to the loss of SMN expression.

On the membrane of lysosomes, mTORC1 works as a sensor for metabolic status, regulating protein and lipid synthesis for cell survival.¹⁴ The local axonal translation in motoneurons is regulated by mTOR signaling.^{15,26} Consistent with a previous report, SMN depletion in NSC-34 cells also resulted in decreased mTOR phosphorylation and its downstream effectors, p70S6K and S6RP (Fig. 5), suggesting that the deac-

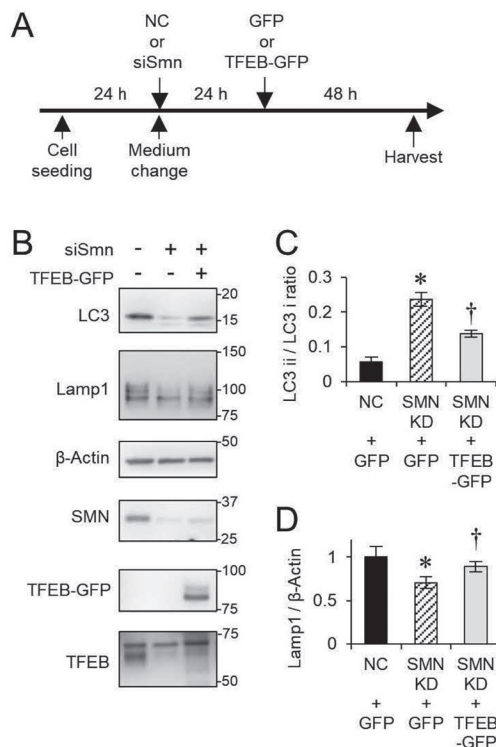


Fig. 4. Exogenous Expression of TFEB Rescues the Depletion SMN in NSC-34 Cells

(A) The experimental design for siRNA and plasmid DNA transfection. After 24 h transfection with either negative control (NC) or SMN (siSmn) siRNA, cells were transfected with either TFEB-GFP or GFP and incubated for an additional 48 h. (B-D) The harvested cell lysates were analyzed by immunoblotting. Representative images are shown in B. The ratio of LC3-ii vs LC3-i and the fold increase in Lamp1 levels, normalized against the β -actin level, are shown in C and D, respectively. $N = 4-5$, mean \pm S.E.M. * $P < 0.05$, Student's t -test vs "NC + GFP". † $P < 0.05$, Student's t -test vs "SMN KD + GFP".

tivation of mTOR might be associated with motoneuron loss in SMA. In addition, axon outgrowth has been reported to be influenced by the PI3K/mTOR pathway,¹²⁾ indicating that mTOR dysfunction in SMA might cause the deterioration of the NMJ. mTOR regulates the activation and nuclear translocation of TFEB.^{12,13)} In the present study, whether the loss of TFEB following SMN KD occurs in an mTOR signaling-dependent manner was not determined. Further investigations are necessary to reveal their causative relationships and roles in motoneurons and SMA pathophysiology.

Several treatments have been approved for SMA. Nusinersen (Spinraza™, Biogen) is an antisense oligo that promotes the production of mature SMN2, including exon 7, by masking the regulatory sequences required for exon 7 splicing, which, consequently, increases the levels of functional SMN protein.³⁴⁾ Onasemnogene Aporavovec-xioi (Zolgensma™, Novartis), also known as AVXS-101, is an Adeno-associated virus 9 that codes the SMN protein, for the replacement of the target gene.³⁵⁾ Although these treatments remediate the defects associated with SMN deficiency, by enhancing SMN levels in the long term, developing new treatments that prevent or reduce neuronal loss would be beneficial for SMA patients. SMA patient-derived pluripotent stem cell-derived cells are useful tools for chemical screening, and some antioxidants have been identified that display protective effects against motoneuron loss.^{36,37)} The aberrant deposition of 4-hydroxy-

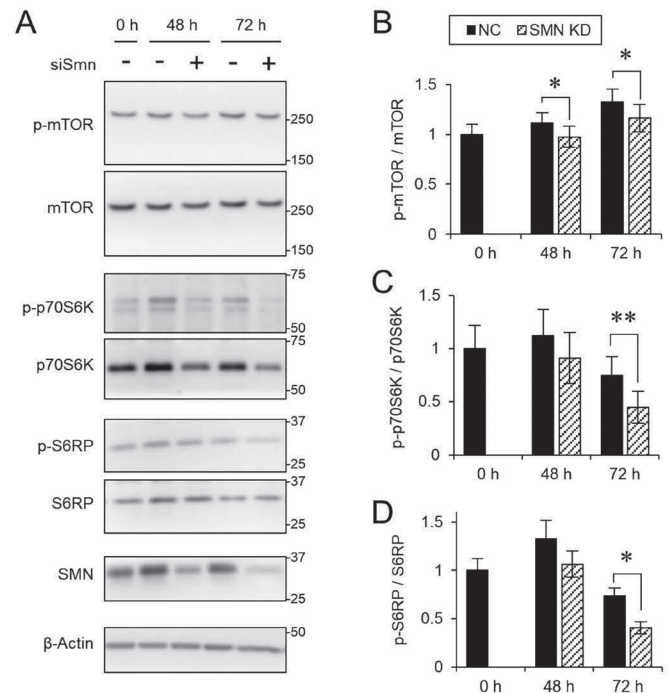


Fig. 5. SMN KD Suppresses mTOR Signaling in NSC-34 Cells

Immunoblotting of cell lysates, obtained from NSC-34 cells, transfected with either negative control (- or NC) or SMN (siSmn + or SMN KD) siRNA, for the indicated times. (A) Representative images of each blot. (B-D) The ratio between the phosphorylated form and the total protein is shown as the fold change relative to the level at 0 h. $N = 5$, mean \pm S.E.M. * $P < 0.05$, ** $P < 0.005$, Student's t -test vs NC.

2-nonenal in spinal motoneurons of SMA patients has been reported,³⁸⁾ and differentiated NSC-34 cells are sensitive to ferroptosis,³⁹⁾ an iron-dependent programmed cell death pathway,⁴⁰⁾ suggesting that motoneurons are relatively sensitive to oxidative stress. Lysosomes and autophagy are responsible for the clearance of lipid peroxides.⁴¹⁾ Motoneurons may display characteristic features that rely on these degradative organelles to reduce oxidative stress, suggesting that chemicals capable of decreasing oxidative stress or increasing the degradation of oxidative-stress-associated molecules may represent drug candidates for SMA.

In conclusion, we demonstrated that SMN regulates the gene expression of TFEB, and consequently, the functions of lysosomes and autophagy. These findings reveal the novel roles of SMN and TFEB during lysosome homeostasis and motoneuron survival.

Acknowledgments This work was Grant-in-Aid for Research Activity Start-up from the Japan Society for Promotion of Science [No. 19K23707 to WO].

Conflict of interest The authors declare no conflict of interest.

REFERENCES

- 1) Crawford TO, Pardo CA. The neurobiology of childhood spinal muscular atrophy. *Neurobiol. Dis.*, **3**, 97–110 (1996).
- 2) Wirth B, Karakaya M, Kye MJ, Mendoza-Ferreira N. Twenty-Five Years of Spinal Muscular Atrophy Research: From Phenotype to

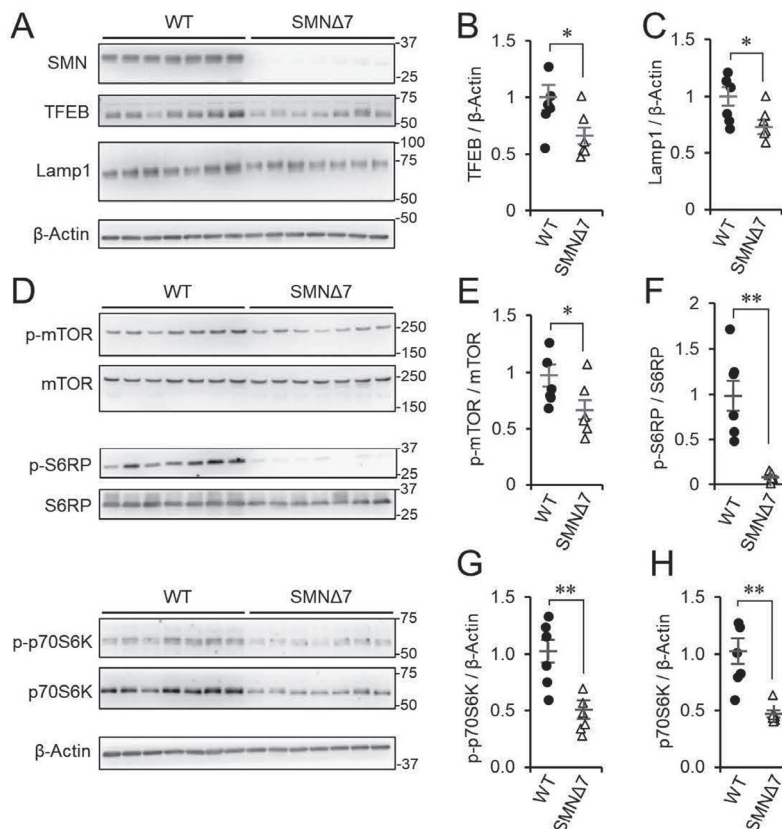


Fig. 6. SMA Model Mice Exhibit Defects in the TFEB and mTOR Pathway, in Lumbar Spinal Cords

A and D show immunoblots for lysates obtained from P11 *SMNΔ7* (*mSmn^{-/-}*, *SMN2^{+/+}*, *SMNΔ7^{+/+}*) and WT (*mSmn^{+/+}*, *SMN2^{+/+}*, *SMNΔ7^{+/+}*) mice. The quantifications of A and D are shown in B–C and E–H, respectively. N = 7, mean ± S.E.M. **P* < 0.05, ***P* < 0.005, Student's *t*-test vs WT.

- Genotype to Therapy, and What Comes Next. *Annu. Rev. Genomics Hum. Genet.* (2020).
- Lorson CL, Hahnen E, Androphy EJ, Wirth B. A single nucleotide in the SMN gene regulates splicing and is responsible for spinal muscular atrophy. *Proc. Natl. Acad. Sci. USA*, **96**, 6307–6311 (1999).
 - Lefebvre S, Bürglen L, Reboullet S, Clermont O, Burlet P, Viollet L, Benichou B, Cruaud C, Millasseau P, Zeviani M. Identification and characterization of a spinal muscular atrophy-determining gene. *Cell*, **80**, 155–165 (1995).
 - Fallini C, Zhang H, Su Y, Silani V, Singer RH, Rossoll W, Bassell GJ. The survival of motor neuron (SMN) protein interacts with the mRNA-binding protein HuD and regulates localization of poly(A) mRNA in primary motor neuron axons. *J. Neurosci.*, **31**, 3914–3925 (2011).
 - Liu Q, Fischer U, Wang F, Dreyfuss G. The spinal muscular atrophy disease gene product, SMN, and its associated protein SIP1 are in a complex with spliceosomal snRNP proteins. *Cell*, **90**, 1013–1021 (1997).
 - Burnett BG, Muñoz E, Tandon A, Kwon DY, Sumner CJ, Fischbeck KH. Regulation of SMN protein stability. *Mol. Cell. Biol.*, **29**, 1107–1115 (2009).
 - Rodriguez-Muela N, Parkhitko A, Grass T, Gibbs RM, Norabuena EM, Perrimon N, Singh R, Rubin LL. Blocking p62-dependent SMN degradation ameliorates spinal muscular atrophy disease phenotypes. *J. Clin. Invest.*, **128**, 3008–3023 (2018).
 - Luzio JP, Pryor PR, Bright NA. Lysosomes: fusion and function. *Nat. Rev. Mol. Cell Biol.*, **8**, 622–632 (2007).
 - Lawrence RE, Zoncu R. The lysosome as a cellular centre for signalling, metabolism and quality control. *Nat. Cell Biol.*, **21**, 133–142 (2019).
 - Sardiello M, Palmieri M, di Ronza A, Medina DL, Valenza M, Gennarino VA, Di Malta C, Donaudy F, Embrione V, Polishchuk RS, Banfi S, Parenti G, Cattaneo E, Ballabio A. A gene network regulating lysosomal biogenesis and function. *Science*, **325**, 473–477 (2009).
 - Roczniak-Ferguson A, Petit CS, Froehlich F, Qian S, Ky J, Angarola B, Walther TC, Ferguson SM. The transcription factor TFEB links mTORC1 signaling to transcriptional control of lysosome homeostasis. *Sci. Signal.*, **5**, ra42 (2012).
 - Settembre C, Zoncu R, Medina DL, Vetrini F, Erdin S, Erdin S, Huynh T, Ferron M, Karsenty G, Vellard MC. Others. A lysosome-to-nucleus signalling mechanism senses and regulates the lysosome via mTOR and TFEB. *EMBO J.*, **31**, 1095–1108 (2012).
 - Liu GY, Sabatini DM. mTOR at the nexus of nutrition, growth, ageing and disease. *Nat. Rev. Mol. Cell Biol.*, **21**, 183–203 (2020).
 - Rehorst WA, Thelen MP, Nolte H, Türk C, Cirak S, Peterson JM, Wong GW, Wirth B, Krüger M, Winter D, Kye MJ. Muscle regulates mTOR dependent axonal local translation in motor neurons via CTRP3 secretion: implications for a neuromuscular disorder, spinal muscular atrophy. *Acta Neuropathol. Commun.*, **7**, 154 (2019).
 - Wang H, Wang R, Xu S, Lakshmana MK. Transcription Factor EB Is Selectively Reduced in the Nuclear Fractions of Alzheimer's and Amyotrophic Lateral Sclerosis Brains, 2016.
 - Cortes CJ, Miranda HC, Frankowski H, Batlevi Y, Young JE, Le A, Ivanov N, Sopher BL, Carrameu C, Muotri AR, Garden GA, La Spada AR. Polyglutamine-expanded androgen receptor interferes with TFEB to elicit autophagy defects in SBMA. *Nat. Neurosci.*, **17**, 1180–1189 (2014).
 - Noda Y, Tsuruma K, Takata M, Ishisaka M, Tanaka H, Nakano Y, Nagahara Y, Shimazawa M, Hara H. GPNMB Induces BiP Expression by Enhancing Splicing of BiP Pre-mRNA during the Endoplasmic Reticulum Stress Response. *Sci. Rep.*, **7**, 12160 (2017).
 - Ohuchi K, Funato M, Yoshino Y, Ando S, Inagaki S, Sato A, Kawase C, Seki J, Saito T, Nishio H, Nakamura S, Shimazawa M, Kaneko H, Hara H. Notch Signaling Mediates Astrocyte Abnormality in Spinal Muscular Atrophy Model Systems. *Sci. Rep.*, **9**, 3701 (2019).

- 20) Otsu W, Ishida K, Nakamura S, Shimazawa M, Tsusaki H, Hara H. Blue light-emitting diode irradiation promotes transcription factor EB-mediated lysosome biogenesis and lysosomal cell death in murine photoreceptor-derived cells. *Biochem. Biophys. Res. Commun.*, **526**, 479–484 (2020).
- 21) Otsu W, Hsu Y-C, Chuang J-Z, Sung C-H. The Late Endosomal Pathway Regulates the Ciliary Targeting of Tetraspanin Protein Peripherin 2. *J. Neurosci.*, **39**, 3376–3393 (2019).
- 22) Cashman NR, Durham HD, Blusztajn JK. Neuroblastoma× spinal cord (NSC) hybrid cell lines resemble developing motor neurons. *Developmental*, (1992).
- 23) Maier O, Böhm J, Dahm M, Brück S, Beyer C, Johann S. Differentiated NSC-34 motoneuron-like cells as experimental model for cholinergic neurodegeneration. *Neurochem. Int.*, **62**, 1029–1038 (2013).
- 24) Wang F, Gómez-Sintes R, Boya P. Lysosomal membrane permeabilization and cell death. *Traffic*, **19**, 918–931 (2018).
- 25) Napolitano G, Ballabio A. TFEB at a glance. *J. Cell Sci.*, **129**, 2475–2481 (2016).
- 26) Kye MJ, Niederst ED, Wertz MH, Gonçalves I do CG, Akten B, Dover KZ, Peters M, Riessland M, Neveu P, Wirth B, Kosik KS, Sardi SP, Monani UR, Passini MA, Sahin M. SMN regulates axonal local translation via miR-183/mTOR pathway. *Hum. Mol. Genet.*, **23**, 6318–6331 (2014).
- 27) Parker GC, Li X, Anguelov RA, Toth G, Cristescu A, Acsadi G. Survival motor Neuron protein regulates apoptosis in an in vitro model of Spinal muscular atrophy. *Neurotox. Res.*, **13**, 39–48 (2008).
- 28) Le TT, Pham LT, Butchbach MER, Zhang HL, Monani UR, Covert DD, Gavrilina TO, Xing L, Bassell GJ, Burghes AHM. SMNΔ7, the major product of the centromeric survival motor neuron (SMN2) gene, extends survival in mice with spinal muscular atrophy and associates with full-length SMN, 2005.
- 29) Cai Q, Sheng Z-H. Molecular motors and synaptic assembly. *Neuroscientist*, **15**, 78–89 (2009).
- 30) Gonzalez Porras MA, Sieck GC, Mantilla CB. Impaired Autophagy in Motor Neurons: A Final Common Mechanism of Injury and Death. *Physiology (Bethesda)*, **33**, 211–224 (2018).
- 31) Song JW, Misgeld T, Kang H, Knecht S, Lu J, Cao Y, Cotman SL, Bishop DL, Lichtman JW. Lysosomal activity associated with developmental axon pruning. *J. Neurosci.*, **28**, 8993–9001 (2008).
- 32) Connolly KJ, O'Hare MB, Mohammed A, Aitchison KM, Anthoney NC, Taylor MJ, Stewart BA, Tuxworth RI, Tear G. The neuronal ceroid lipofuscinosis protein Cln7 functions in the postsynaptic cell to regulate synapse development. *Sci. Rep.*, **9**, 15592 (2019).
- 33) Willett R, Martina JA, Zewe JP, Wills R, Hammond GRV, Puertollano R. TFEB regulates lysosomal positioning by modulating TMEM55B expression and JIP4 recruitment to lysosomes. *Nat. Commun.*, **8**, 1580 (2017).
- 34) Singh NK, Singh NN, Androphy EJ, Singh RN. Splicing of a critical exon of human Survival Motor Neuron is regulated by a unique silencer element located in the last intron. *Mol. Cell. Biol.*, **26**, 1333–1346 (2006).
- 35) Hensel N, Kubinski S, Claus P. The Need for SMN-Independent Treatments of Spinal Muscular Atrophy (SMA) to Complement SMN-Enhancing Drugs. *Front. Neurol.*, **11**, 45 (2020).
- 36) Ando S, Funato M, Ohuchi K, Kameyama T, Inagaki S, Seki J, Kawase C, Tsuruma K, Shimazawa M, Kaneko H, Hara H. Edaravone is a candidate agent for spinal muscular atrophy: *in vitro* analysis using a human induced pluripotent stem cells-derived disease model. *Eur. J. Pharmacol.*, **814**, 161–168 (2017).
- 37) Ando S, Funato M, Ohuchi K, Inagaki S, Sato A, Seki J, Kawase C, Saito T, Nishio H, Nakamura S, Shimazawa M, Kaneko H, Hara H. The Protective Effects of Levitetacetam on a Human iPSCs-Derived Spinal Muscular Atrophy Model. *Neurochem. Res.*, **44**, 1773–1779 (2019).
- 38) Hayashi M, Araki S, Arai N, Kumada S, Itoh M, Tamagawa K, Oda M, Morimatsu Y. Oxidative stress and disturbed glutamate transport in spinal muscular atrophy. *Brain Dev.*, **24**, 770–775 (2002).
- 39) Martinez AM, Mirkovic J, Staniszc ZA, Patwari FS, Yang WS. NSC-34 motor neuron-like cells are sensitized to ferroptosis upon differentiation. *FEBS Open Bio*, **9**, 582–593 (2019).
- 40) Dixon SJ, Lemberg KM, Lamprecht MR, Skouta R, Zaitsev EM, Gleason CE, Patel DN, Bauer AJ, Cantley AM, Yang WS, Morrison B 3rd, Stockwell BR. Ferroptosis: an iron-dependent form of nonapoptotic cell death. *Cell*, **149**, 1060–1072 (2012).
- 41) Pivtoraiko VN, Stone SL, Roth KA, Shacka JJ. Oxidative stress and autophagy in the regulation of lysosome-dependent neuron death. *Antioxid. Redox Signal.*, **11**, 481–496 (2009).